Mn-enhanced MRI for early tumor detection and in vivo growth rate analysis in a mouse medulloblastoma model

Giselle A. Suero-Abreu[1,2], G. Praveen Raju[3], Orlando Aristizabal[1], Eugenia Volkova[1], Edward J. Houston[1], Diane Pham[3], Alexandre Wojcinski[4], Kamila U. Szulc[1], Daniel Colon[1], Alexandra L. Joyner[4], and Daniel H. Turnbull[1,2]

[1]*Skirball Institute of Biomolecular Medicine, NYU School of Medicine, NY, NY, United States,* [2]*Department of Radiology, NYU School of Medicine, NY, NY, United States,* [3]*Department of Pediatrics, Weill Cornell Medical College, NY, NY, United States,* [4]*Developmental Biology Program, Sloan-Kettering Institute, Memorial Sloan-Kettering Cancer Center, NY, NY, United States*

Target Audience: This study will be of interest to those using MRI to analyze tumor progression in pre-clinical mouse models, and to those applying Mn-enhanced MRI (MEMRI) for anatomical and functional imaging in the mouse brain.

Purpose: Genetically-engineered mouse models have been critical for understanding brain tumor formation and progression[1]. In the case of medulloblastoma (MB), the most common malignant pediatric brain tumor that occurs in the cerebellum, mouse models have transformed our understanding of the molecular origins and heterogeneity of MB subtypes[2-4]. MRI is an important tool for both clinical diagnosis and pre-clinical monitoring of brain tumor progression and response to therapy. We have previously shown that Mn-enhanced MRI (MEMRI) is a powerful approach for in vivo analysis of mouse cerebellum development[5,6], and that MEMRI can be used to detect and monitor cerebellar tumor progression in a *Ptch1* conditional knockout (*Ptch1*-CKO) mouse model of sporadic MB[7]. The current study aimed to establish MEMRI for early MB detection, and to characterize growth of early MBs in *Ptch1*-CKO mice.

Methods: ***Animal model****: Ptch1* gene function was removed in relatively few, isolated *Ptf1a*-expressing granule cell precursors (GCPs) to generate the *Ptch1*-CKO MB model[7]. ***MRI****:* All MRI was performed on a 7T Biospec scanner (Bruker) using a 25-mm (ID) quadrature Litz coil (Doty). MR images were acquired from anaesthetized mice (1.0-1.5% isoflurane in air), 24h after intra-peritoneal injection of $MnCl_2$ (80 mg/kg for mice up to 1 month of age; 100 mg/kg for mice older than 1 month). MEMRI images were acquired with 3D T1-weighted GE sequences for high-throughput screening (TE/TR=4/15-ms, flip angle=18°, matrix=128^3 giving 150-µm isotropic resolution in 15 min), and high-resolution imaging (TE/TR=3.6/50-ms, flip angle=40º, matrix=256^3 giving 100-µm isotropic resolution in 1h 49 min). T2-weighted images were also acquired using a multi-slice (6 500-µm thick slices) RARE sequence (TE/TR=8.9/4000-ms, Effective TE=35-ms, RARE factor=8, matrix=256^2 giving 80-µm in-plane resolution in 9 min). ***Image analysis:*** 3D segmentation and rendering of tumor volumes was performed using Amira software (Visage Imaging). For each mouse, tumor volumes were fitted to an exponential growth model: Volume = $V_0 \bullet \exp(bT)$, where T is the time in weeks, V_0 is the initial volume (at birth, T=0), and the exponent b was used as an effective measure of growth rate. ***Histology:*** After imaging, selected mice were cardio-perfused with paraformaldehyde, and their brains were harvested, embedded in paraffin and sectioned at 7-µm thickness. Serial H&E stained sections were used to confirm the MEMRI results and to validate the 3D renderings generated from MRI data.

Results: MEMRI enhancement was evident in the internal granule cell layer (IGL) but not the external granule layer (EGL) or tumors, which therefore presented with negative contrast to the surrounding normal cerebellum. Compared to conventional tumor imaging methods, MEMRI was able to detect early pre-neoplastic lesions (thickened EGL, 100-200 µm) at 2 weeks, which could not be seen on RARE images (Fig. 1; N=12 validated with histology). The 3D spatial distribution of these histology-validated early lesions was examined (Fig. 2), showing that most connected lesions were bilateral at 2-3 weeks (N=6/12) compared to unilateral (N=2/12), and there were also several mice with multiple lesions (N=4/12). All of the lesions had a predominant anterior component (N=12), while many also had a (smaller) posterior component (N=8/12). Lesion / tumor volume was measured as a function of age between 3 to 20 weeks, and fit to exponential curves to measure growth rate (Fig. 3, N=28). MB growth rates were heterogeneous in the *Ptch1*-CKO mouse model, from slow to fast, and included several examples where early lesions regressed and disappeared with age (N=6).

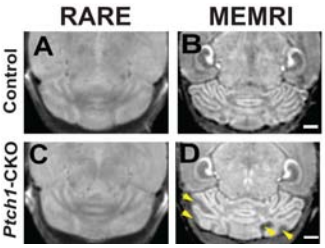

Fig. 1: RARE vs MEMRI of (A,B) normal (control) cerebellum and (C,D) lesions (arrows) in *Ptch1*-CKO mice.

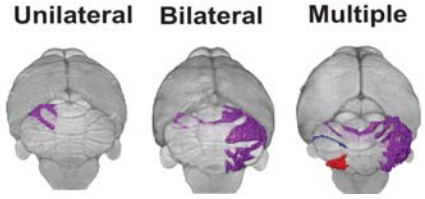

Fig. 2: Distributions of early lesions in *Ptch1*-CKO mice: unilateral (2/12), bilateral (6/12) and multiple (4/12) lesions (color-coded).

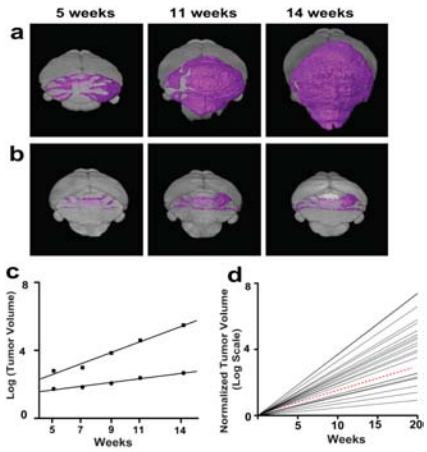

Fig. 3: Fast (a) and slow (b) tumor growth in two *Ptch1*-CKO mice. (c) Quantitative volume data fitted to exponential curves for the mice in (a and b). (d) Exponential growth curves for 22 mice, including the mean growth curve (dashed red).

Discussion and Conclusion: These results show that MEMRI provides a powerful method for longitudinal imaging of MB progression in the mouse brain, allowing early detection and in vivo analysis of tumor growth rates. The ability to detect pre-neoplastic lesions as early as 2 weeks makes it feasible to use MEMRI to follow the fates of individual lesions that either regress or progress to overt MB tumors. Previously, MEMRI was used to guide micro-array analysis of advanced MBs in *Ptch1*-CKO mice, demonstrating the presence of at least 2 distinct molecular phenotypes in these tumors[7]. In future studies, it will be interesting to perform similar analyses to assess molecular signatures that may be associated with fast and slow progressing MB tumors.

References: **1.**Fomchenko & Holland, Clin Cancer Res 2006, 12:5288-97; **2.**Gilbertson & Ellison, Annu Rev Pathol 2008, 3:341-85; **3.**Markant & Wechsler-Reya, Neuropathol Appl Neurobiol 2012, 38:228-40; **4.**Northcott *el al*., Nat Rev Cancer 2012, 12:818-34; **5.**Wadghiri *et al.*, NMR Biomed 2004, 17:613-19; **6.**Szulc *et al*., Magn Reson Med 2013, doi:10.1002/mrm.24597 [Epub ahead of print]; **7.**Suero-Abreu *et al.*, Proc ISMRM 2012, 20:169. ***Acknowledgements:*** This research was supported by NIH grants R01NS038461 (DHT), R01HL078665 (DHT), R01CA128158 (ALJ), and K08NS066083 (GPR), and a Geoffrey Beene Cancer Research Center grant 21680 (ALJ).